Hindawi
Journal of Nanomaterials
Volume 2022, Article ID 7255181, 10 pages
https://doi.org/10.1155/2022/7255181

Research Article

Optimized Synthesis of Xanthan gum/ZnO/ TiO_2 Nanocomposite with High Antifungal Activity against Pathogenic *Candida albicans*

Fatemeh Ghorbani,[1] **Pourya Gorji**,[1] **Mohammad Salmani Mobarakeh**,[2] **Hamid Reza Mozaffari**,[3] **Reza Masaeli**,[4] **and Mohsen Safaei**[2,5]

[1]*Students Research Committee, Kermanshah University of Medical Sciences, Kermanshah, Iran*
[2]*Advanced Dental Sciences Research Center, Kermanshah University of Medical Sciences, Kermanshah, Iran*
[3]*Department of Oral and Maxillofacial Medicine, School of Dentistry, Kermanshah University of Medical Sciences, Kermanshah, Iran*
[4]*Department of Dental Biomaterials, School of Dentistry, Tehran University of Medical Sciences, Tehran, Iran*
[5]*Division of Dental Biomaterials, School of Dentistry, Kermanshah University of Medical Sciences, Kermanshah, Iran*

Correspondence should be addressed to Mohsen Safaei; mohsen_safaei@yahoo.com

Received 20 November 2021; Revised 5 March 2022; Accepted 30 March 2022; Published 25 April 2022

Academic Editor: Seyed alireza Hashemi

Increased resistance of fungal pathogens to common antimicrobial agents is known as one of the most important human problems. Due to the limited variety of antifungal drugs available, the identification and use of new antifungal drugs are essential. This study aimed to determine the optimal conditions for synthesizing a novel nanocomposite of xanthan gum/ZnO/ TiO_2 with the highest antifungal activity against *Candida albicans* (*C. albicans*). For this purpose, nine experiments were designed using the Taguchi method. In the designed experiments, three factors of xanthan gum, ZnO, and TiO_2 nanoparticles have been investigated at three different levels, and the best ratio with the highest antifungal activity was determined. The results showed that in the presence of the synthesized nanocomposite in experiment 3 (xanthan gum 0.01 M, ZnO 0.09 M, and TiO_2 0.09 M), the inhibition of fungal growth reached 92.51%. The properties of the synthesized nanocomposite and its components were investigated using different characterization methods, which confirmed the formation of nanocomposites with desirable properties. The antifungal activity results showed that the synthesized nanocomposite as an antifungal agent has an effective performance and can be used well in various fields.

1. Introduction

The dramatic increase in microbial resistance to antimicrobials has become a pervasive challenge and a serious threat to public health worldwide. *C. albicans* is one of the most common fungal pathogens in humans. The widespread use of a limited number of antifungal agents has led to drug resistance in treating *C. albicans* infections, a problem that is becoming increasingly important [1]. The range of human infections caused by the *C. albicans* yeast and several related species is significant. They cause various infection levels, from relatively trivial conditions such as oral candidiasis and genital infections to fatal and systemic infections in patients who have already had serious illnesses. There has been great interest in fighting *Candida* infections, especially *C. albicans*, as fatal infections have become more common and new disorders have been identified with *Candida* [2].

Antifungal drugs often belong to two groups of polyenes and azoles. These compounds act on fungal cells by disrupting the metabolism of RNA or DNA and causing intracellular accumulation of peroxide. The currently available antifungal agents used topically and systemically to treat *C. Albicans* have shown serious side effects that have greatly limited their use. Toxicity and drug resistance are the main

reasons for extensive research on new antifungal compounds [3]. Since discovering and using a new class of antimicrobial compounds is very time-consuming, expensive, and usually unsuccessful, an alternative is to use modern science and design and synthesize compounds with antimicrobial properties. Nanotechnology has solved many current problems by using structures with at least one dimension of 1 to 100 nanometers [4–6]. In recent years, significant studies have been conducted in applications of nanomaterials, and their effectiveness has been observed in many fields. Metal oxides with antimicrobial properties are among the most widely used compounds in various fields [6, 7]. The use of nanomaterials can be effective in combating fungal infections. Due to their special properties, such as proper penetration into target cells and tissues, these particles have been able to provide more inhibitory power with lower concentrations compared to conventional compounds [8].

Extensive sources of zinc metal, reasonable price, antimicrobial, antioxidant, and anticancer properties make zinc a valuable metal as a raw material in the production of various compounds such as mouthwashes and toothpaste that reduce plaque and bad breath [9, 10]. ZnO nanoparticles have successfully inhibited pathogenic microbes such as *Streptococcus mutans* and *Staphylococcus aureus* [11].

Titanium dioxide (TiO_2) has unique properties such as high photocatalytic activity, anticancer, antimicrobial properties, biocompatibility, reactivity, cheap and safe production, nontoxicity, temperature stability, and chemical stability [12, 13]. These properties of TiO_2 are used in the production of food, pharmaceutical, biomedicine, environment, cosmetics, air purification, water disinfection, solar cell production, and antimicrobial compounds [14]. It is an optical catalyst whose antimicrobial applications have been investigated more than any other material with this property [15]. TiO_2NPs can inactivate microorganisms and exhibit antimicrobial properties by producing hydroxyl free radicals and superoxide [16, 17].

Similar properties are found in natural materials. Xanthan gum is a type of polysaccharide that is naturally produced by the *Xanthomonas* bacterium [18]. Its main chain consists of β-D-glucose units interconnected in positions 1 and 4; in addition, two mannose and glucuronic acid are also involved in its structure [19]. Among the desirable properties of xanthan are nontoxic, inexpensive, with high biocompatibility, thermal stability, resistance to acid and base, high stability and solubility in water, and antimicrobial properties [20, 21].

Due to the tendency of nanoparticles to agglomerate, which leads to the loss of their desirable properties, it is necessary to use strategies to prevent this. The use of nanoparticles in the form of nanocomposites can largely prevent them from agglomerating. For this purpose, this study was designed and conducted for the first time to determine the optimal conditions for the synthesis of xanthan gum/ZnO/$TiO_2$with the highest antifungal properties.

2. Materials and Methods

2.1. TiO_2 Nanoparticle Synthesis. To prepare TiO_2NPs using the sol-gel method, 10 ml of isopropanol was combined with 10 ml of deionized water, and 20 ml of titanium isopropoxide solution was added dropwise with continuous stirring. The resulting solution was placed at 60 °C for 60 min, the yellow gel formed in the oven was dried at 80 °C, and the gel powder was calcined in air for 3 h at 650 °C [22].

2.2. ZnO Nanoparticle Synthesis. Zinc acetate ($Zn(CH_3CO_2)_2{\cdot}2H_2O$) and sodium hydroxide (NaOH) were used to prepare ZnO nanoparticles. First, 0.1 M zinc acetate and 0.2 M sodium hydroxide solutions were prepared by dissolving them in deionized water.

Then two solutions were poured into a beaker and stir at 750 rpm for 2 h at 60 °C. After 2 h, a clear milky white solution was formed. The next step was centrifugation at 5000 rpm for 5 min to precipitate a white product. The precipitate was washed first with deionized water and then with acetone. ZnO NPs were obtained in powder form by drying the product using an oven at 75 °C for 6 h [23].

2.3. Xanthan Gum/ZnO/TiO_2 Nanocomposite Synthesis. To determine the optimal conditions for the synthesis of xanthan gum/ZnO/TiO_2 nanocomposite with the highest antimicrobial activity, using Qulitek-4 software according to the Taguchi method, 9 experiments containing different ratios of xanthan gum, ZnO, and titanium NPs were designed. To evaluate the antimicrobial activity of synthesized nanocomposites, using in situ method and 0.01, 0.02, and 0.03 M levels of xanthan gum and 0.03, 0.06, and 0.09 M levels of ZnO and TiO_2 NPs, nine samples of nanocomposites were tested. To synthesize the studied nanocomposite, xanthan gum was prepared commercially; ZnO and TiO_2NPs were prepared by coprecipitation and sol-gel methods, respectively. In the synthesis of nanocomposites, first, the solutions of the components were stirred separately by a magnetic stirrer for one h. All three solutions were then dispersed at room temperature for 15 min using an ultrasonic homogenizer. Finally, solutions of ZnO and TiO_2NPs were added simultaneously and dropwise to the solution containing xanthan gum. The final solutions were stirred for one h and then dispersed for 15 min by an ultrasonic homogenizer. Finally, the prepared solution was placed in an oven at 60 °C for 24 h to form nanocomposite sediments. The resulting precipitate was separated from the container with a spatula and ground in a mortar to prepare the final nanocomposite powder [24].

2.4. Antifungal Activity. The antifungal activity of synthesized xanthan gum/ZnO/TiO_2 nanocomposites on *C. albicans* (ATCC 10231) was studied using the colony forming unit (CFU) method. For this purpose, *C. albicans* was incubated on a Sabouraud dextrose agar (SDA) medium for 48 h at 37 °C to prepare an isolated colony. After that, a colony was taken and dissolved in twice distilled water to obtain an approximate 10^6 CFU/ml concentration. To evaluate the antifungal activity of the synthesized nanocomposites, solutions containing SDA and 9 synthesized nanocomposites (1 mg/ml) were prepared. The resulting solutions were poured into the Petri dish, and after freezing the culture medium, 100 μL of the fungal suspension prepared on the

Table 1: Taguchi design of experiments and fungal growth inhibition rate of xanthan/ZnO/TiO_2 synthesized nanocomposite.

Experiment	Xanthan gum (M)			ZnO (M)			TiO_2 (M)			Fungal growth inhibition (%)
	0.01	0.02	0.03	0.03	0.06	0.09	0.03	0.06	0.09	
1		0.01			0.03			0.03		61.73
2		0.01			0.06			0.06		84.11
3		0.01			0.09			0.09		92.51
4		0.02			0.03			0.06		75.64
5		0.02			0.06			0.09		88.32
6		0.02			0.09			0.03		81.17
7		0.03			0.03			0.09		72.98
8		0.03			0.06			0.03		69.44
9		0.03			0.09			0.06		90.47

Table 2: The main effects of different levels of xanthan gum, ZnO, and TiO_2on growth inhibition of *Candida albicans*.

Factors	Level 1	Level 2	Level 3
Xanthan gum	79.45	81.71	77.63
ZnO	70.12	80.62	88.05
TiO_2	70.78	83.41	84.60

Table 3: The interactions effects of studied factors on growth inhibiting of *Candida albicans*.

Interacting factor pairs	Column	Severity index (%)	Optimum conditions
Xanthan gum × TiO_2	1 × 3	45.33	[1,3]
Xanthan gum × ZnO	1 × 2	15.75	[1,3]
ZnO × TiO_2	2 × 3	1.23	[3,3]

culture medium was completely cultured using a swap. In the control group, 100 μL of fungal suspension was cultured on a pure SDA medium. The number of colonies was counted for 9 experimental and control groups after 96 h of incubation at 28 °C. The inhibition of fungal growth by each of the synthesized nanocomposites is calculated using the following equation:

$$\text{Growth fungus inhibition rate}\,(\%) = \frac{\text{Cg} - \text{Eg}}{\text{Cg}} \times 100, \quad (1)$$

where Cg is the average growth of colonies in the control group and Eg is the average growth in the experimental group. Thus, the optimal conditions for synthesizing nanocomposites with the highest antifungal activity were determined from 9 experiments. All experiments were repeated three times.

2.5. Characterization. The properties of the synthesized nanocomposite and its components were investigated using different characterization methods, including Fourier transforms infrared (FTIR) spectroscopy (Thermo Company at RT, USA), X-ray diffraction (XRD) (Philips X'Pert (40 kV, 30 mA), The Netherlands), field emission scanning electron microscope (FESEM) (TESCAN Company, MIRA III model, Czech Republic), SAMX detector (France) on FESEM, transmission electron microscope (TEM) (TEM Philips EM208S, The Netherlands), ultraviolet-visible (UV-Vis) spectroscopy (Shimadzu Company UV-160 A model, Japan), and thermal analysis (TGA-DTA) (TA Company, Q600 model).

Table 4: The analysis of variance of factors affecting the growth inhibition of *Candida albicans*.

Factors	DOF	Sum of squares	Variance	F ratio (F)	Pure sum	Percent (%)
Xanthan gum	2	25.07	12.53	15.93	23.49	2.71
ZnO	2	487.15	243.57	309.61	485.57	56.09
TiO_2	2	351.95	175.97	223.68	350.38	40.47

DOF, degree of freedom.

Table 5: The optimum conditions for the synthesis of xanthan/ZnO/TiO_2 nanocomposite with the highest antifungal activity.

Factors	Level	Contribution
Xanthan gum	2	2.11
ZnO	3	8.45
TiO_2	3	5.01
Total contribution from all factors		15.57
Current grand average of performance		79.60
Fungal growth inhibition at optimum condition		95.17

3. Results and Discussion

3.1. Antifungal Activity. Optimal conditions for the production of xanthan gum/ZnO/TiO_2 nanocomposites with the highest antifungal activity were determined based on 9 experiments designed by the Taguchi method. Table 1 shows the effect of nanocomposites synthesized under different conditions on the growth inhibition of *C. albicans*. The results showed that the nanocomposites produced in

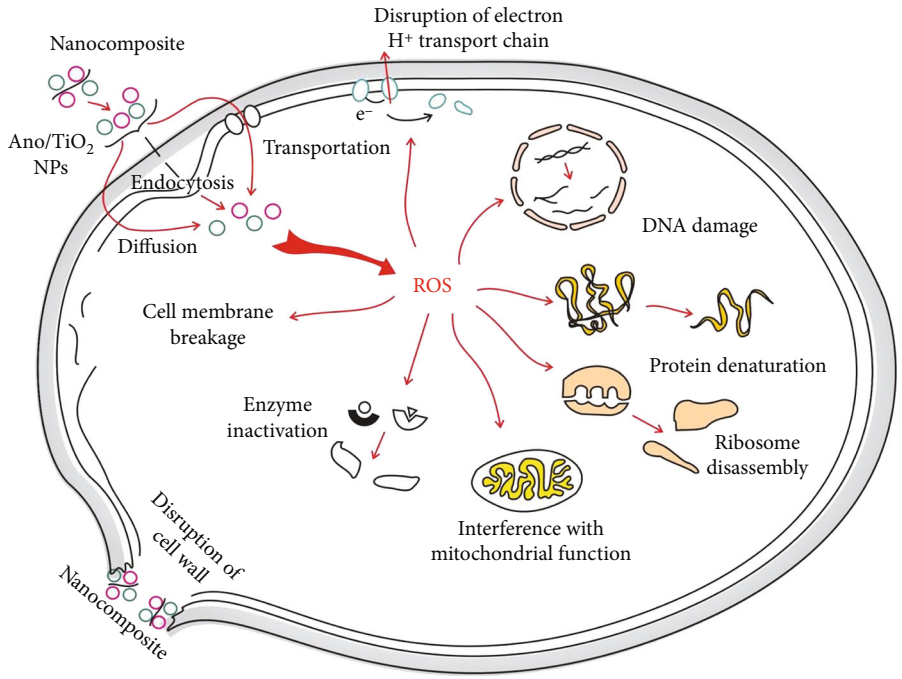

Figure 1: Schematic mechanisms for antifungal activity of xanthan gum/ZnO/TiO_2nanocomposite.

experiment 3 (xanthan gum 0.01 M, ZnO NPs 0.09 M, and TiO_2NPs 0.09 M) had the highest antifungal activity against *C. albicans* and, under those conditions, the highest inhibition of fungal growth (92.51%) occurred.

Table 2 shows the effect of xanthan gum, ZnO, and TiO_2NPs factors on the growth inhibition of *C. albicans*. The results indicate that the xanthan gum factor at level 2 and ZnO and TiO_2 NPs at level 3 had the greatest effect in inhibiting the growth of *C. albicans*.

The interaction of factors on the growth inhibition of *C. albicans* is presented in Table 3. Xanthan gum in the first level and TiO_2 in the third level had the most interaction and the growth inhibition of *C. albicans* at 45.33%. Xanthan gum in the first level and ZnO in the third level showed a significant interaction on the growth inhibition of *C. albicans* by 15.75%. The lowest percentage of interaction intensity index belonged to ZnO and TiO_2 in the third level at 1.23%.

The analysis of variance of the parameters affecting the growth inhibition of *C. albicans* is presented in Table 4. The highest effect on inhibiting the growth of *C. albicans* was shown by ZnO with an effect of 56.09%, TiO_2 by 40.47%, and xanthan gum by 2.71%, respectively.

After reviewing the data and analyzing the effect of each factor and their interaction, the optimal conditions for the synthesis of xanthan gum/ZnO/TiO_2 nanocomposite with the highest antifungal activity were estimated (Table 5). Based on these results, ZnO had the highest contribution, and xanthan gum had the lowest contribution in inhibiting the growth of *C. albicans*, and TiO_2 showed an effect between these two factors and close to ZnO. The second level was the most appropriate level for the xanthan gum factor and the third level for ZnO and TiO_2NPs factors. Based on the results, it was estimated that the synthesized nanocomposite in optimal conditions inhibited about 95% of fungal growth, which was most consistent with the results of experiment 3.

Previous similar studies have reported the optimal antimicrobial properties of nanomaterials and their components. Nanoparticles currently used in the clinical field are limited by agglomeration. Many studies have used the modification of impurities and the synthesis of nanocomposites to prevent nanoparticles from agglomerating and disperse nanoparticles in different environments. In other words, the modification in this way is one of the most effective ways to regulate and control the interaction of nanoparticles and germs [25–28].

The larger area and high density of nanoparticles allow them to show antimicrobial activity more favorably on the surface of fungi with more interaction. In addition, nanoparticles combined with polymers or coated on the surfaces of biocompatible materials have been used to improve their antimicrobial properties. The study of the mechanism of antimicrobial activity of nanocomposites containing metal oxides indicates that these nanostructures can cause the destruction of the fungal cell wall and the penetration of nanoparticles into the cell. Nanoparticles that pass through the cell wall are not fully understood. However, their transport, diffusion and endocytosis, and entry into the cell can lead to the production of reactive oxygen species (ROS) and thus interfere with the function of many intracellular organs [29, 30]. Reactive oxygen species seem to play a major role in antifungal activity. By inducing oxidative stress, they can destroy all biomolecules in the cell (including proteins and DNA) and disrupt the function of intracellular organs [31]. Nanostructures can also cause fungal death by damaging cellular enzymes and disrupting the electron transfer chain (Figure 1).

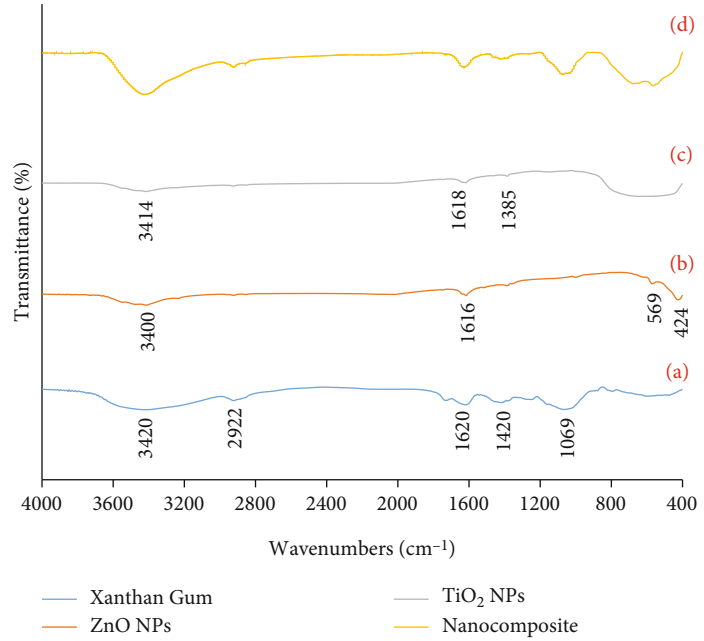

Figure 2: FTIR spectra of xanthan gum (a), ZnO NPs (b), TiO_2 NPs (c), and xanthan Gum/ZnO/TiO_2 nanocomposite (d).

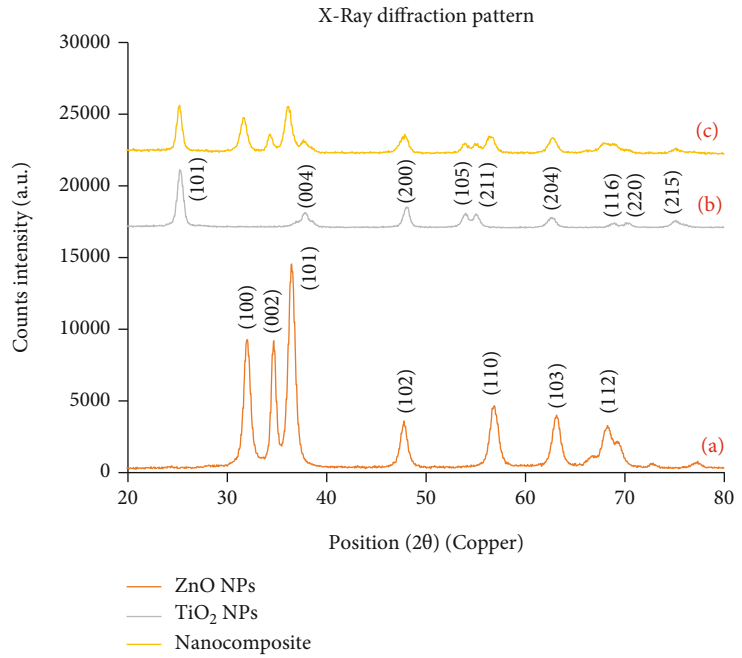

Figure 3: XRD Pattern of ZnO NPs (a), TiO_2 NPs (b), and xanthan gum/ZnO/TiO_2 nanocomposite (c).

3.2. FTIR Analysis. The FTIR spectra of xanthan gum (diagram a), ZnO NPs (diagram b), TiO_2 nanoparticles (diagram c), and synthesized nanocomposites (diagram d), in the wavelength range of 400-4000 cm^{-1}, are shown in Figure 2.

In the FTIR spectrum of xanthan gum (diagram a), two peaks at positions 3420 and 2922 cm^{-1} were observed for the tensile bonds of -OH and -CH, respectively. Asymmetric and symmetric tensile vibrations related to carboxylate group -COO- bonds were shown at 1620 and 1420 cm^{-1}, respectively. A wide absorption peak was observed at 1069 cm^{-1} due to the tensile vibration of the glycosidic bond [32].

In the FTIR spectrum of ZnO NPs (diagram b), a wide adsorption peak in the range of 3100-3700 cm^{-1} was observed for the tensile bonds of O-H due to residual alcohols, water, and Zn-OH bond. The flexural state was shown in the H-OH bond of the ZnO NPs at the 1616 cm^{-1} position. The strongest wide adsorbed band was observed at

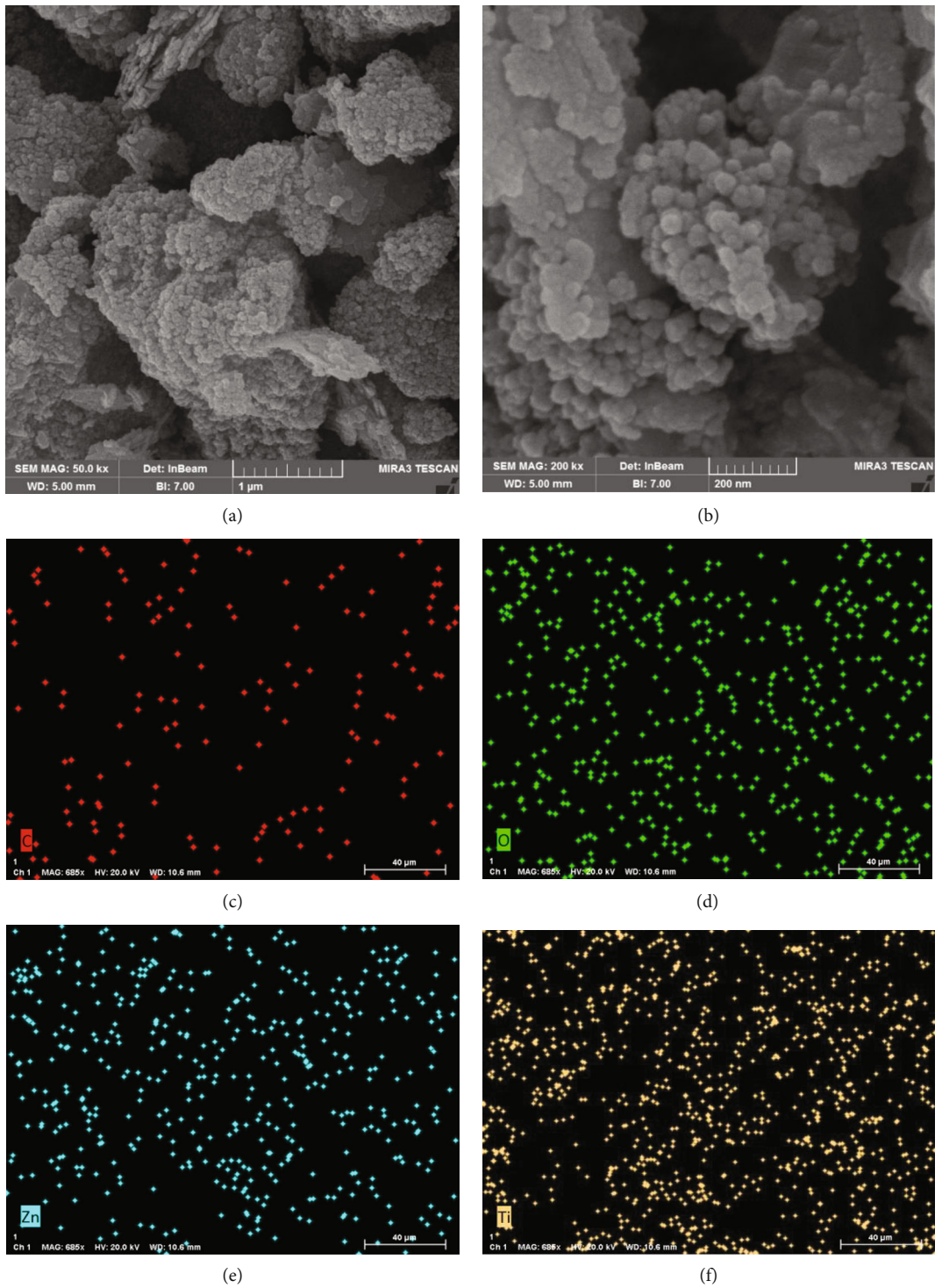

Figure 4: The scanning electron microscope images of xanthan gum/ZnO/TiO_2 nanocomposite at different magnification (a, b) and corresponding energy-dispersive X-ray spectroscopy (EDS) elemental mapping for C (c), 4O (d), Ti (e), and Zn (f).

424 cm^{-1} due to the tensile vibrations related to oxygen and zinc. Zn-O tensile bands were observed at 424 and 569 cm^{-1} for pure samples of ZnO NPs [33].

In the FTIR spectrum of TiO_2 nanoparticles (diagram c), the peaks observed at 3414 cm^{-1} and 1635 cm^{-1} refer to the adsorbed moisture and the O-H surface groups. The peak observed in the 1618 cm^{-1} region corresponds to the bending vibrations of the water molecule, and the peak index of the 1385 cm^{-1} region is due to the carbonate group, which is created by the adsorption of ambient carbon dioxide by nanoparticles. Sharp peaks observed in the range below 850 cm^{-1} showed the binding of oxygen to titanium [34, 35]. The peaks

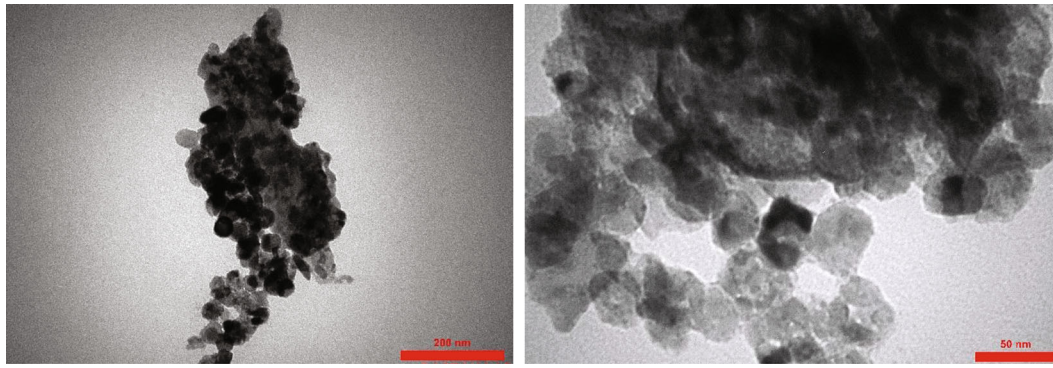

Figure 5: The transmitted electron microscope images of xanthan gum/ZnO/TiO_2 nanocomposite at different magnification.

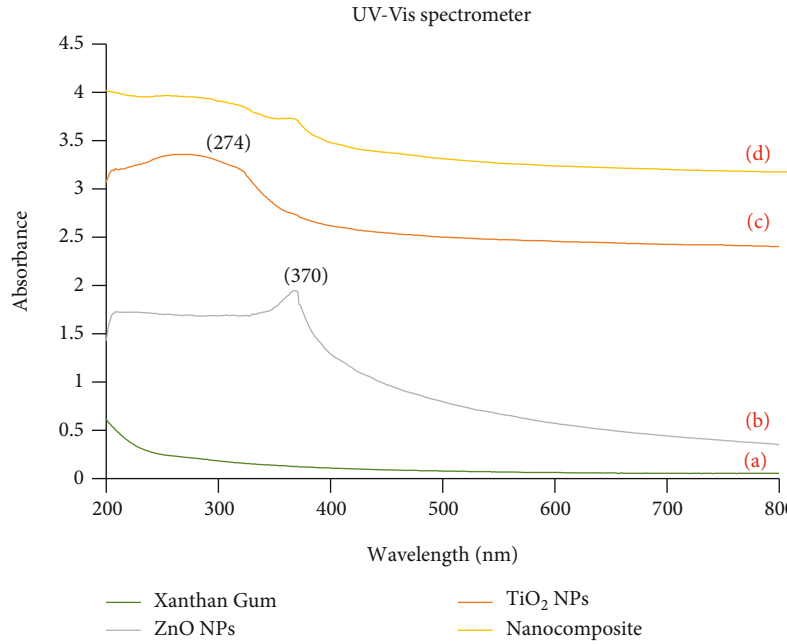

Figure 6: UV-visible of xanthan gum (a), ZnO NPs (b), TiO_2 NPs (c), and xanthan gum/ZnO/TiO_2 nanocomposite (d).

observed in the final nanocomposite spectrum (diagram d) showed a combination of peaks in the xanthan gum spectrum and oxide nanoparticles. Therefore, the strong interactions between the components and the formation of the final nanocomposite were confirmed [24].

3.3. XRD Analysis. The X-ray diffraction pattern of Figure 3 is presented to investigate the crystal structure and to identify ZnO NPs (diagram a), TiO_2 nanoparticles (diagram b), and synthesized nanocomposites (diagram c). The X-ray diffraction pattern of ZnO NPs (diagram a) showed the hexagonal crystal structure of the zincite phase for these nanoparticles. Miller indices of (hkl), (100), (002), (101), (102), (110), (103), and (112) were calculated at angles 2θ, 32, 35, 37, 48, 57, 63, and 68 degrees, respectively [36].

The X-ray diffraction pattern of TiO_2NPs (diagram b) showed the anatase phase with a tetragonal crystal structure for this material. Miller indices (hkl), (101), (004), (200), (105), (211), (204), (116), (220), and (215) were calculated at angles 2θ, 25, 38, 48, 54, 55, 63, 69, 70. and 75 degrees, respectively [37].

X-ray diffraction pattern obtained from synthesized nanocomposite (diagram c) showed the presence of component peaks and their intensity reduction, flattening or removal, and displacement of some peaks relative to the X-ray diffraction pattern of components in the synthesized nanocomposite X-ray diffraction spectrum. In addition, the average crystallite size was calculated for the highest peak of 28 nm.

3.4. SEM and Elemental Mapping Analysis. The appearance and elemental mapping of the xanthan gum/ZnO/TiO_2 nanocomposite were examined by field emission scanning electron microscopy (Figure 4). Figures 4(a) and 4(b) show the placement of metal oxide nanoparticles inside the xanthan gum, resulting in the formation of the final nanocomposite. Elemental mapping was performed by energy-dispersive X-ray spectroscopy (EDS) to evaluate the

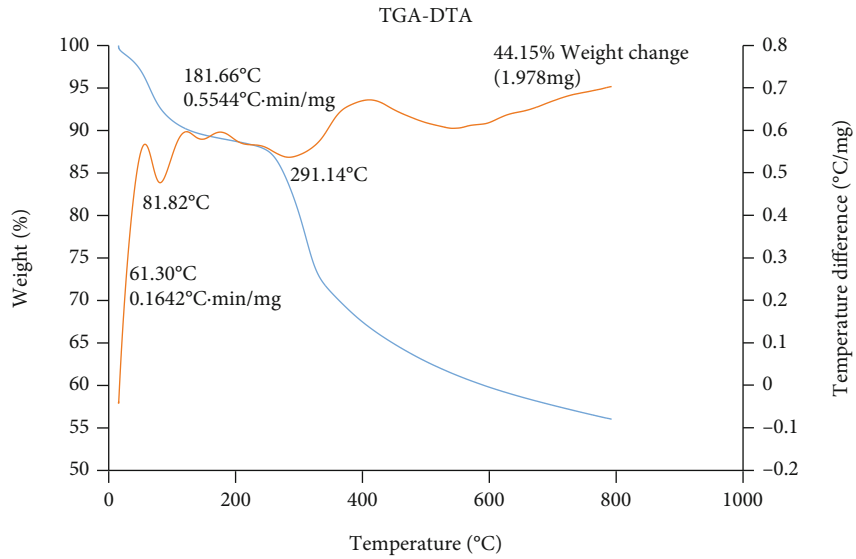

Figure 7: Thermogravimetric analysis (TGA-DTA) of xanthan gum/ZnO/TiO_2 nanocomposite.

elemental dispersion in the xanthan gum/ZnO/TiO_2 nanocomposite. Figures 4(c) to 4(f) shows that elements C, O, Zn, and Ti are regularly distributed, confirming the suitable synthesis of the xanthan gum/ZnO/TiO_2 nanocomposite.

3.5. TEM Analysis. The morphology of the xanthan gum/ZnO/TiO_2nanocomposite was investigated by TEM micrograph preparation of the synthesized nanocomposite. TEM micrograph analysis showed the formation of this nanocomposite (Figure 5). The morphology and distribution of oxide nanoparticles were also examined in more detail by TEM. The results showed that the metal oxide nanoparticles were well in contact with the xanthan gum and the final nanocomposite was prepared by distributing different sizes of particles.

3.6. UV-Vis Analysis. The optical properties of xanthan gum/ZnO/TiO_2nanocomposite and its components were investigated using ultraviolet-visible spectroscopy in the range of 200 to 800 nm (Figure 6). No specific absorption band was observed in the xanthan gum spectrum (diagram a). In the spectrum of ZnO NPs (diagram b), a sharp and specific peak showed the production of adsorption in the range of 370 nm for this sample. In the spectrum of TiO_2NPs (diagram c), a wide absorption band with the highest intensity in the range of 274 nm was observed. The absorption spectra of the final synthesized nanocomposite (diagram d) showed the presence of a wide low-intensity absorption peak in the range of 270 nm and a specific low-intensity peak in the range of 371 nm. This confirmed the interaction of the components of the nanocomposite [24].

3.7. Thermal analysis. The thermal properties of xanthan gum/ZnO/TiO_2nanocomposite composition and its thermal stability were evaluated by TGA and DTA analysis (Figure 7). The behavior of thermogravimetric analysis and differential thermal analysis of the final nanocomposite showed the three main stages of weight loss by 44.15%. The first stage, consisting of 11% weight loss, occurred in the range of 25–250 °C due to the moisture loss and dehydration of the prepared nanocomposite. The second stage, with a weight loss of 28%, in the temperature range of 250-550 °C, is related to the thermal decomposition of the elements of impurity components and carbon bonds in the nanocomposite. In the last stage of weight loss, with a weight loss of 5.15%, in the temperature range of 550-800 °C, the structural water, which is in the form of bonded hydroxyl groups, begins to decompose and release. In addition, at this stage, impurities with higher thermal stability were decomposed. In the diagram obtained from the differential thermal analysis of the final nanocomposite, exothermic peaks were observed upwards, and endothermic peaks were observed downwards.

4. Conclusions

By analyzing the results of experiments designed by the Taguchi method, the antifungal activity of xanthan gum/ZnO/TiO_2nanocomposite synthesized by in situ method against *C. albicans* fungal strains was evaluated. The optimal antifungal properties of synthesized nanocomposite were confirmed. Based on the antifungal activity results, it was estimated that the synthesized nanocomposite under the optimal conditions prevents fungal growth up to 95%. Due to the antifungal properties predicted for this nanocomposite, its use as an antimicrobial agent in medicine and dentistry can be effectively useful, and it dramatically reduces pathogenic microbes. Identifying and synthesizing novel and effective antimicrobial compounds can reduce the prevalence of many microbial diseases and prevent increased treatment costs. It is recommended that clinical studies be performed locally and systemically to evaluate the effectiveness of this nanocomposite in the treatment of oral and vaginal candidiasis.

Data Availability

The data used to support the findings of this study are included within the article.

Conflicts of Interest

The authors declare that they have no conflicts of interest.

Acknowledgments

This work was supported by grant number 990429 from the Kermanshah University of Medical Sciences.

References

[1] A. Zida, S. Bamba, A. Yacouba, R. Ouedraogo-Traore, and R. Guiguemdé, "Substances naturelles actives sur _Candida albicans_ , sources de nouveaux medicaments antifongiques : revue de la litterature," *Journal de MycologieMedicale*, vol. 27, no. 1, pp. 1–19, 2017.

[2] M. McCullough, B. Ross, and P. Reade, "_Candida albicans_ : a review of its history, taxonomy, epidemiology, virulence attributes, and methods of strain differentiation," *International Journal of Oral and Maxillofacial Surgery*, vol. 25, no. 2, pp. 136–144, 1996.

[3] J. A. Parente-Rocha, A. M. Bailão, A. C. Amaral et al., "Antifungal resistance, metabolic routes as drug targets, and new antifungal agents: an overview about endemic dimorphic fungi," *Mediators of Inflammation*, vol. 2017, Article ID 9870679, 2017.

[4] R. Rezaei, M. Safaei, H. R. Mozaffari et al., "The role of nanomaterials in the treatment of diseases and their effects on the immune system," *Open Access Macedonian Journal of Medical Sciences*, vol. 7, no. 11, pp. 1884–1890, 2019.

[5] H. Moradpoor, M. Safaei, F. Rezaei et al., "Optimisation of cobalt oxide nanoparticles synthesis as bactericidal agents," *Open Access Macedonian Journal of Medical Sciences*, vol. 7, no. 17, pp. 2757–2762, 2019.

[6] S. El-Sayed, M. Amer, T. Meaz, N. Deghiedy, and H. El-Shershaby, "Microstructure optimization of metal oxide nanoparticles and its antimicrobial activity," *Measurement*, vol. 151, article 107191, 2020.

[7] M. Taran, M. Safaei, N. Karimi, and A. Almasi, "Benefits and application of nanotechnology in environmental science: an overview," *Biointerface Research in Applied Chemistry*, vol. 11, no. 1, pp. 7860–7870, 2021.

[8] A. León-Buitimea, J. A. Garza-Cervantes, D. Y. Gallegos-Alvarado, M. Osorio-Concepción, and J. R. Morones-Ramírez, "Nanomaterial-based antifungal therapies to combat fungal diseases aspergillosis, Coccidioidomycosis, Mucormycosis, and candidiasis," *Pathogens*, vol. 10, no. 10, p. 1303, 2021.

[9] S. Keerthana and A. Kumar, "Potential risks and benefits of zinc oxide nanoparticles: a systematic review," *Critical Reviews in Toxicology*, vol. 50, no. 1, pp. 47–71, 2020.

[10] H. Moradpoor, M. Safaei, H. R. Mozaffari et al., "An overview of recent progress in dental applications of zinc oxide nanoparticles," *RSC Advances*, vol. 11, no. 34, pp. 21189–21206, 2021.

[11] E. Schifano, D. Cavallini, G. De Bellis et al., "Antibacterial effect of zinc oxide-based nanomaterials on environmental biodeteriogens affecting historical buildings," *Nanomaterials*, vol. 10, no. 2, p. 335, 2020.

[12] H. M. Ali, H. Babar, T. R. Shah, M. U. Sajid, M. A. Qasim, and S. Javed, "Preparation techniques of TiO_2 nanofluids and challenges: a review," *Applied Sciences*, vol. 8, no. 4, p. 587, 2018.

[13] M. Catauro, E. Tranquillo, G. Dal Poggetto, M. Pasquali, A. Dell'Era, and S. Vecchio Ciprioti, "Influence of the heat treatment on the particles size and on the crystalline phase of TiO2 synthesized by the sol-gel method," *Materials*, vol. 11, no. 12, p. 2364, 2018.

[14] C. L. de Dicastillo, C. Patiño, M. J. Galotto et al., "Novel hollow titanium dioxide nanospheres with antimicrobial activity against resistant bacteria," *Beilstein Journal of Nanotechnology*, vol. 10, no. 1, pp. 1716–1725, 2019.

[15] S. Mathew, P. Ganguly, V. Kumaravel et al., "Effect of chalcogens (S, Se, and Te) on the anatase phase stability and photocatalytic antimicrobial activity of TiO2," *Materials Today: Proceedings*, vol. 33, pp. 2458–2464, 2020.

[16] G. De Falco, A. Porta, P. Del Gaudio, M. Commodo, P. Minutolo, and A. D'Anna, "Antimicrobial activity of TiO 2 coatings prepared by direct thermophoretic deposition of flame-synthesized nanoparticles," *MRS Advances*, vol. 2, no. 28, pp. 1493–1498, 2017.

[17] C. Liao, Y. Li, and S. C. Tjong, "Visible-light active titanium dioxide nanomaterials with bactericidal properties," *Nanomaterials*, vol. 10, no. 1, p. 124, 2020.

[18] D. R. A. Muhammad, A. S. Doost, V. Gupta et al., "Stability and functionality of xanthan gum–shellac nanoparticles for the encapsulation of cinnamon bark extract," *Food Hydrocolloids*, vol. 100, article 105377, 2020.

[19] M. K. Schnizlein, K. C. Vendrov, S. J. Edwards, E. C. Martens, and V. B. Young, "Dietary xanthan gum alters antibiotic efficacy against the murine gut microbiota and attenuates Clostridioides difficile colonization," *Msphere*, vol. 5, no. 1, pp. 708–719, 2020.

[20] M. H. A. Elella, M. Sabaa, D. H. Hanna, M. M. Abdel-Aziz, and R. R. Mohamed, "Antimicrobial pH-sensitive protein carrier based on modified xanthan gum," *Journal of Drug Delivery Science and Technology*, vol. 57, article 101673, 2020.

[21] Z. Wang, Q. Yang, X. Wang et al., "Antibacterial activity of xanthan-oligosaccharide against Staphylococcus aureus via targeting biofilm and cell membrane," *International Journal of Biological Macromolecules*, vol. 153, pp. 539–544, 2020.

[22] A. Karami, "Synthesis of TiO 2 nano powder by the sol-gel method and its use as a photocatalyst," *Journal of the Iranian Chemical Society*, vol. 7, no. S2, pp. S154–S160, 2010.

[23] R. E. Adam, G. Pozina, M. Willander, and O. Nur, "Synthesis of ZnO nanoparticles by co-precipitation method for solar driven photodegradation of Congo red dye at different pH," *Photonics and Nanostructures - Fundamentals and Applications*, vol. 32, pp. 11–18, 2018.

[24] M. Safaei, M. Taran, L. Jamshidy et al., "Optimum synthesis of polyhydroxybutyrate-Co_3O_4 bionanocomposite with the highest antibacterial activity against multidrug resistant bacteria," *International Journal of Biological Macromolecules*, vol. 158, pp. 477–485, 2020.

[25] B. Das, M. I. Khan, R. Jayabalan et al., "Understanding the antifungal mechanism of Ag@ZnO core-shell nanocomposites against Candida krusei," *Scientific Reports*, vol. 6, no. 1, p. 36403, 2016.

[26] S. Wang, J. Wu, H. Yang, X. Liu, Q. Huang, and Z. Lu, "Antibacterial activity and mechanism of Ag/ZnO nanocomposite

against anaerobic oral pathogen Streptococcus mutans," *Journal of Materials Science: Materials in Medicine*, vol. 28, no. 1, p. 23, 2017.

[27] S. Gharpure, A. Akash, and B. Ankamwar, "A review on antimicrobial properties of metal nanoparticles," *Journal of Nanoscience and Nanotechnology*, vol. 20, no. 6, pp. 3303–3339, 2020.

[28] A. I. Raafat, N. M. El-Sawy, N. A. Badawy, E. A. Mousa, and A. M. Mohamed, "Radiation fabrication of xanthan-based wound dressing hydrogels embedded ZnO nanoparticles: in vitro evaluation," *International Journal of Biological Macromolecules*, vol. 118, Part B, pp. 1892–1902, 2018.

[29] N. N. Ilkhechi, M. Mozammel, and A. Y. Khosroushahi, "Antifungal effects of ZnO, TiO_2 and ZnO- TiO_2 nanostructures on _Aspergillus flavus_," *Pesticide Biochemistry and Physiology*, vol. 176, article 104869, 2021.

[30] M. Safaei, M. Taran, and M. M. Imani, "Preparation, structural characterization, thermal properties and antifungal activity of alginate-CuO bionanocomposite," *Materials Science and Engineering C*, vol. 101, pp. 323–329, 2019.

[31] T. R. Lakshmeesha, M. Murali, M. A. Ansari et al., "Biofabrication of zinc oxide nanoparticles from _Melia azedarach_ and its potential in controlling soybean seed-borne phytopathogenic fungi," *Saudi Journal of Biological Sciences*, vol. 27, no. 8, pp. 1923–1930, 2020.

[32] M. H. A. Elella, E. S. Goda, H. M. Abdallah, A. E. Shalan, H. Gamal, and K. R. Yoon, "Innovative bactericidal adsorbents containing modified xanthan gum/montmorillonite nanocomposites for wastewater treatment," *International Journal of Biological Macromolecules*, vol. 167, pp. 1113–1125, 2021.

[33] P. G. Devi and A. S. Velu, "Synthesis, structural and optical properties of pure ZnO and co doped ZnO nanoparticles prepared by the co-precipitation method," *Journal of Theoretical and Applied Physics*, vol. 10, no. 3, pp. 233–240, 2016.

[34] A. Fahami, R. Ebrahimi-Kahrizsangi, and B. Nasiri-Tabrizi, "Mechanochemical synthesis of hydroxyapatite/titanium nanocomposite," *Solid State Sciences*, vol. 13, no. 1, pp. 135–141, 2011.

[35] R. B. KC, C. K. Kim, M. S. Khil, H. Y. Kim, and I. S. Kim, "Synthesis of hydroxyapatite crystals using titanium oxide electrospun nanofibers," *Materials Science and Engineering: C*, vol. 28, no. 1, pp. 70–74, 2008.

[36] S. Getie, A. Belay, A. Chandra Reddy, and Z. Belay, "Synthesis and characterizations of zinc oxide nanoparticles for antibacterial applications," *Journal of Nanomedicine and Nanotechnology*, vol. s8, p. 004, 2017.

[37] X. Wei, G. Zhu, J. Fang, and J. Chen, "Synthesis, characterization, and photocatalysis of well-dispersible phase-pure anatase TiO_2 nanoparticles," *International Journal of Photoenergy*, vol. 2013, Article ID 726872, 2013.